JACS
JOURNAL OF THE AMERICAN CHEMICAL SOCIETY
Communication
pubs.acs.org/JACS

Reuleaux Triangle Disks: New Shape on the Block

Choon Hwee Bernard Ng and Wai Yip Fan*

Department of Chemistry, National University of Singapore, 3 Science Drive 3, Singapore 117543

Supporting Information

ABSTRACT: We report here the unprecedented preparation of Reuleaux triangle disks. The hydrolysis and precipitation of bismuth nitrate in an ethanol–water system with 2,3-bis(2-pyridyl)pyrazine yielded basic bismuth nitrate Reuleaux triangle disks. Analysis of the intermediates provided insights into the mystery behind the formation of the Reuleaux triangle disk, revealing a unique growth process. The report of a facile method to prepare crystals of a novel shape in high yield, with good homogeneity, and with excellent reproducibility is expected to unlock new research directions in multiple disciplines.

Geometric shapes with high degrees of symmetry have always fascinated the man on the street by the beauty of its simplicity and scientists by the interconnections between structure and function. This structure–function relation is the driving force for discovering and characterizing nanomaterials with novel shapes. It has been demonstrated that, in the nanoscale regime, physical and chemical properties of a material are often intimately linked to its shape. For instance, anisotropic silver (Ag) and gold (Au) nanocrystals exhibit additional scattering peaks not observed for their spherical counterparts, due to localized charge polarizations at vertices.[1,2] Similarly, platinum (Pt) and palladium (Pd) nanocrystals of varied shapes possess different catalytic properties depending on the exposed facets and the number of step edges and kink sites.[3]

Over the past two decades, researchers have developed methods for the preparation of nanocrystals exhibiting a wide range of geometric shapes: triangular and hexagonal prisms, rods and wires, polyhedrons, and multipod structures.[4,5] With the explosion of research and publications in the field, one would assume that most if not all of the possible geometric shapes that can be adopted by crystals have already been uncovered. Herein, we report the first synthesis of Reuleaux triangle disks. Using a solution phase method, basic bismuth nitrate Reuleaux triangle disks can be prepared in high yields, with good homogeneity, and with excellent reproducibility. Despite the plethora of methods developed for shape-controlled synthesis of crystals, the attainment of the Reuleaux triangle shape is unprecedented to the best of our knowledge. In fact, the manifestation of the Reuleaux triangle shape has never even been observed in natural systems.

A Reuleaux triangle (named after German engineer Franz Reuleaux for his work on developing it as a useful mechanical form) is a geometric shape of constant width, in which the separation of two parallel lines tangent to the curve is independent of their orientation (Figure 1A).[6] It is constructed from arcs of circles centered at the vertices of an equilateral

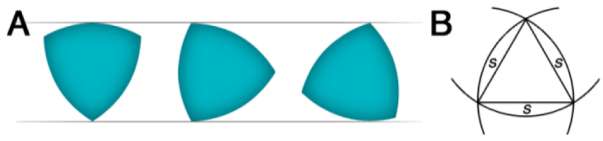

Figure 1. Diagram illustrating (A) the constant width property and (B) construction of the Reuleaux triangle.

triangle (Figure 1B). By the Blaschke–Lebesgue theorem, the Reuleaux triangle has the smallest area of any curve of given constant width, which is given by $(1/2)[\pi - (3)^{1/2})s^2$, where s is the constant width. With the combination of symmetry elegance and functionality, the shape has been applied in a range of functions from guitar picks to drill bits and manhole covers.[7]

Basic bismuth nitrates (BBNs) are compounds that contain Bi^{3+}, NO_3^-, and O^{2-}. The use of BBNs in medicine dates back to the Middle Ages, where they were first administered for treatment of dyspepsia under the trade names *magisterium bismuti* and *bismutum subnitricum*.[8] It was later prescribed as a mild antiseptic and antisyphilitic.[9] BBNs are still used today as a pharmaceutical ingredient for the eradication of Heliobacter pylori bacterium.[10] Prepared from the hydrolysis of aqueous bismuth nitrate, a range of BBNs of similar compositions can be obtained depending on the extent of hydrolysis.[11] Many of such compounds contain hexanuclear polycations of the general formula $[Bi_6O_{4+x}(OH)_{4-x}]^{(6-x)+}$, which is believed to form from the intramolecular condensation of hydrated Bi^{3+} ions.[12] At present, only a handful of these compounds have been structurally characterized by single-crystal X-ray diffraction studies. The lack of progress in this aspect stems from the difficulty in isolation of pure phases, the frequent appearance of twin-crystals and superstructures, as well as the large difference in the X-ray scattering abilities between heavy bismuth and lighter oxygen or nitrogen atoms.[13,14] BBN crystals with largely irregular forms and a sprinkle of nanorods and hexagonal nanoplates have been reported using a microemulsion method.[15]

In our work, the preparation of BBN Reuleaux triangle disks was achieved by the simultaneous hydrolysis and precipitation of bismuth nitrate pentahydrate $Bi(NO_3)_3{\cdot}5H_2O$ in an ethanol–water solvent system with 2,3-bis(2-pyridyl)pyrazine (dpp) as the shape-directing agent. Parts A and B of Figure 2

Received: July 14, 2014
Published: July 29, 2014

   dx.doi.org/10.1021/ja506625y | J. Am. Chem. Soc. 2014, 136, 12840–12843

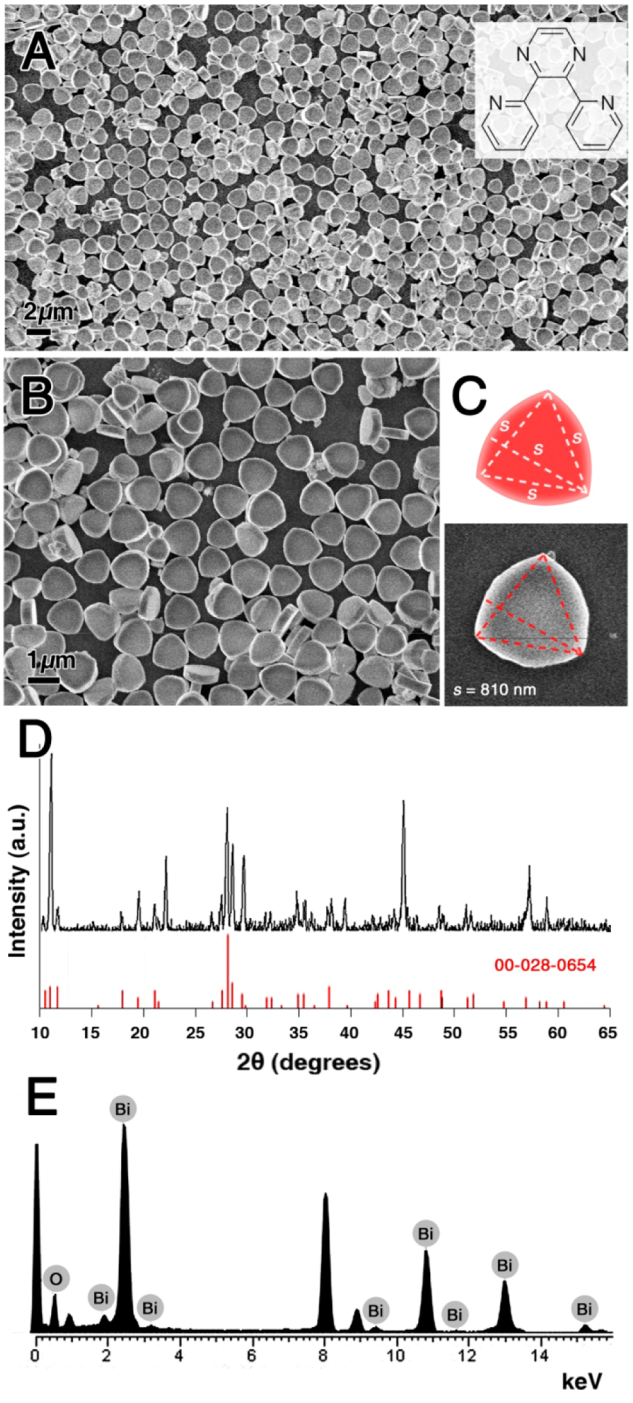

Figure 2. (A, B) SEM images of Reuleaux triangle disks. Inset: structure of dpp. (C) Illustration and corresponding SEM image of a single disk exhibiting the Reuleaux triangle shape. (D) XRD and (E) EDX spectra of Reuleaux triangle disks. XRD reflections are matched to $Bi_6(NO_3)_4(OH)_2O_6{\cdot}2H_2O$ (JCPDS 00-028-0654). The unlabeled peaks in the EDX plot are Cu signals which belong to the Cu grid used for nanoparticle deposition.

show the scanning electron microscope (SEM) images of the BBN crystals. As represented in Figure 2C, the as-obtained crystals have well-defined facets with a Reuleaux triangle disk shape with lengths of ~800 nm. The thickness of the disks was ~200 nm, as observed from disks that were assembled in an upright manner on the substrate (Figure S1A, Supporting Information). The planar morphology was confirmed from angled SEM profiles of the disks (Figure S1B, Supporting Information).

The identity of the as-prepared products was determined by powder X-ray diffraction (XRD) to be $Bi_6(NO_3)_4(OH)_2O_6{\cdot}2H_2O$ (JCPDS 00-028-0654) (Figure 2D). Unfortunately, this analogue of BBN has not been fully characterized by single crystal X-ray diffraction measurements. Work is in progress to obtain single crystals for this compound to fully resolve its structure. Energy dispersive X-ray (EDX) measurements revealed the presence of Bi and O (Figure 2E). The N signals could have been enveloped by the stronger O signal in its vicinity. Bismuth oxide was ruled out as the identity of the disks, as the XRD spectrum did not show any peaks from the different polymorphs. Besides, nanoscale Bi_2O_3 exists as a yellow solid[16] which is different from the white precipitate we obtained.

The morphology and crystal structure of the Reuleaux triangle disks were further characterized by transmission electron microscopy (TEM) and high resolution TEM (HRTEM). As shown in Figure 3A and C, the faceted disks

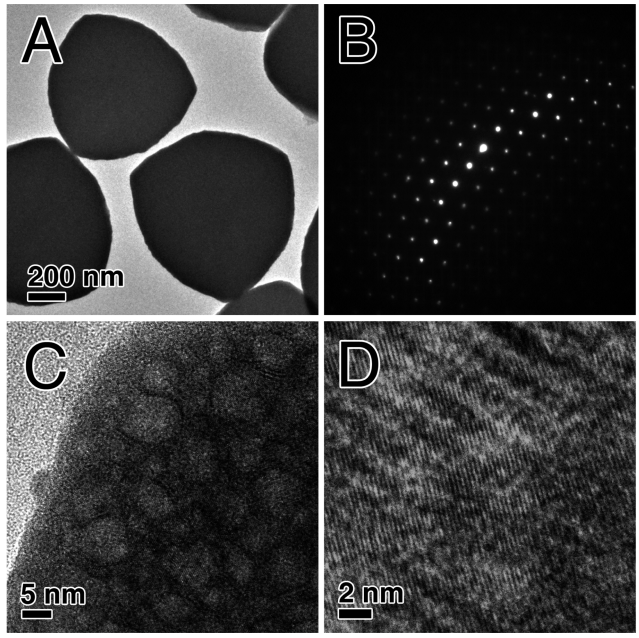

Figure 3. (A) TEM image of Reuleaux triangle disks. (B) SAED patterns obtained from a single disk. (C, D) HRTEM images of a single disk showing the presence of mesopores and crystallographically continuous lattice fringes.

are mesoporous with cavities of ~5 nm. The selected area electron diffraction (SAED) pattern obtained for a single disk consists of a hexagonal array of spots, indicating the single crystalline feature of the BBN crystals (Figure 3B). This is confirmed through HRTEM imaging where uniform lattice fringes were observed (Figure 3D).

Controlled experiments were carried out to investigate the influence of dpp on the formation of the Reuleaux triangle disks, in which dpp was omitted as well as replaced with similar organic molecules such as 2,2′-bipyridyl and pyrazine. As shown in Figure S2 (Supporting Information), the products obtained for all three experiments were hexagonal plates with diameters of 700−800 nm and a thickness of ~100 nm. Powder XRD analyses of the products confirmed the identities of the plates to be $Bi_6(NO_3)_4(OH)_2O_6{\cdot}2H_2O$. Same as for the

dx.doi.org/10.1021/ja506625y | J. Am. Chem. Soc. 2014, 136, 12840−12843

Reuleaux triangle disks, HRTEM imaging of the plates revealed a single crystalline structure consisting of irregular mesopores (Figure S3, Supporting Information). These results suggest that dpp plays a crucial role for the formation of the Reuleaux triangle disks.

To gain insight into the mechanistic basis behind this unusual growth of Reuleaux triangle morphology, we attempted to monitor the reaction products at various reaction times. Under typical experimental conditions, Reuleaux triangle disks were formed in less than 60 s, which made following the growth process difficult. However, we discovered that, by limiting the amount of water added to the system, the growth of the Reuleaux triangle disks can be arrested. SEM imaging of the as-obtained products in the controlled experiment showed a spectrum of partially formed disks (Figure S4, Supporting Information). Through a thorough inspection of the intermediates frozen in the various stages of formation, vital insights into the growth process and mechanism could be elucidated. Figure 4 illustrates the growth process of the

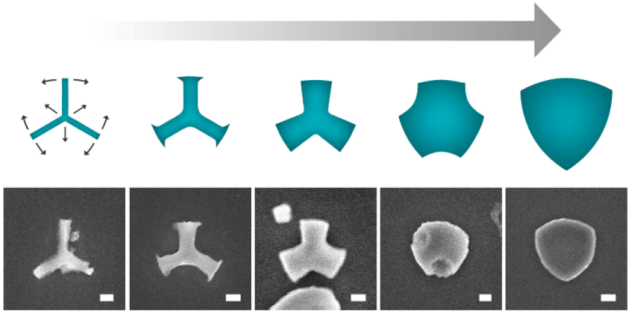

Figure 4. Scheme illustrating the growth process of Reuleaux triangle disks. Arrows indicate the apparent growth directions. Scale bars = 100 nm.

Reuleaux triangle disks. Planar tripods were formed initially, and further growth occurred with each pod extending in both directions along an arc as well as radically outward toward the eventual vertices of the Reuleaux triangle.

At present, there are two widely accepted crystal growth mechanisms. In the classical crystallization model, atoms/ions are added successively to a primary particle to form a single crystal,[17] while, in the nonclassical model, primary particles aggregate in an oriented fashion to form single-crystalline secondary structures.[18] This spontaneous oriented attachment is thermodynamically driven in the substantial reduction in surface free energy arising from the elimination of high energy surfaces.[19] From TEM images of the intermediate structures (Figure S5, Supporting Information), it is evident that the Reuleaux triangle disks grew from a nonclassical nanoparticle-based aggregation pathway. Nucleation of BBN first produced 10 nm single-crystalline nanoparticles which first underwent random aggregation to produce polycrystalline intermediates. Subsequent realignment and crystallographic fusion resulted in the formation of single crystalline disks with mesoporous architectures (i.e., oriented attachment mechanism).[20]

The exact mechanism for the growth of the Reuleaux triangle shape is still under investigation. However, we believe that it formed under the interplay of organic additive-directed growth and mesoscopic transformation in a confined reaction environment (Figure 5). The synthesis of the BBN plates is similar to that of the reprecipitation method to prepare organic nanoparticles.[21,22] The method involves rapid mixing of a

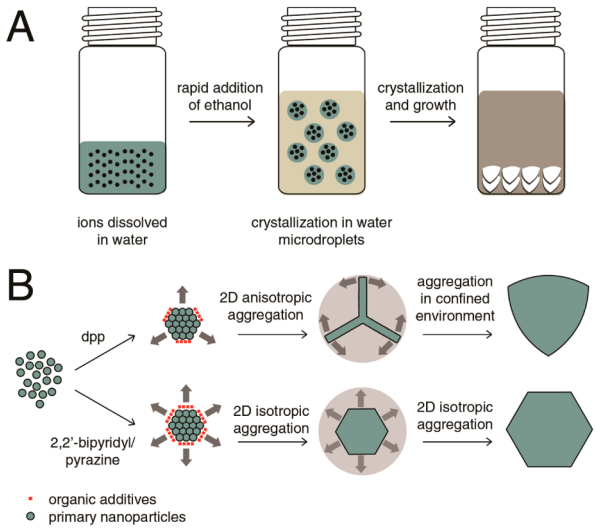

Figure 5. Scheme illustrating the mechanism for the formation of Reuleaux triangle disks: (A) Rapid addition of ethanol leads to the formation of aqueous microdroplets within which nucleation and growth occurs. (B) Different pathways of crystal growth under the influence of organic additives. For dpp, selective adsorption on the sides of the hexagon aggregate leads to anisotropic 2D growth into planar tripods until it reaches the boundary of the microdroplet. Subsequent growth follows a curved trajectory under continuous modulation by dpp and confinement effects. For 2,2′-bipyridyl and pyrazine, nonselective adsorption leads to isotropic 2D growth into larger hexagonal nanoplates. Block arrows indicate the growth directions.

solution of the organic compound dissolved in a good solvent with excess of a poor solvent. For the method to work, there must exist a disparity in solubility of the organic compound in the two solvents and the two solvents must be miscible.

In our case, BBN is known to be insoluble in ethanol.[23] The rapid mixing of ethanol and the bismuth nitrate solution results in a change in the microenvironment of the ions, giving rise to microdroplets within which the ions are confined.[24] The instantaneous exposure to the poor solvent surroundings induces the supersaturation and formation of BBN nanoparticles in the microdroplets. Further aggregation and mesoscopic transformations then take place in the confined environment (Figure 5A).

To account for the structural intermediates observed in our work, we propose that small hexagonal aggregates could have formed in the early stages of aggregation, under the influence of the inherent crystal structure. This hypothesis may be supported by the formation of hexagonal plates when the synthesis was carried out in the absence of organic modifiers. It is known that, in the absence of organic additives, the morphology of the final product is largely determined by the anisotropic nature of the building units.[25,26] Furthermore, early work on BBN also reported the observation of hexagonal crystals.[27] As observed for several systems, these hexagonal plates could be bound by a mixture of facets on alternate side faces which can lead to anisotropic 2D growth.[28,29]

The ability of organic additives in effecting anisotropic growth has been extensively studied and can be explained by the specific adsorption on particular facets therefore inhibiting growth by lowering their surface energy.[30] As illustrated in Figure 4B, dpp could have been selectively adsorbed on the sides of the hexagonal aggregates, directing further aggregation

dx.doi.org/10.1021/ja506625y | J. Am. Chem. Soc. 2014, 136, 12840−12843

in an anisotropic 2D fashion to give the trigonal planar intermediates. Similar 2D anisotropic growth has also been reported to yield planar tripods.[29] Further outward growth is halted on reaching the boundary of the microdroplet, and subsequent aggregation is forced to occur within the confined environment. Under the continuous modulation of dpp-mediated aggregation and boundary confinement, the growth of the intermediate follows a curved trajectory toward the formation of Reuleaux triangle disks.

In the case of 2,2′-bipyridyl and pyridine, nonselective adsorption on the hexagonal aggregates would give rise to isotropic 2D growth to larger hexagonal plates to an equilibrium size modulated by the confined reaction environment (Figure 5B). This process is consistent with the observation of polydispersed hexagonal disks obtained for the experiment where the growth was arrested with the addition of limited amounts of water. Although it is not possible to determine the size of the microbubbles, the similar sizes of the Reuleaux triangle and hexagonal disks are consistent with confined spaces of 800−900 nm in diameter.

The report of a facile method to prepare Reuleaux crystals in high yields, good homogeneity, and excellent reproducibility may be expected to stimulate computer simulation of this unique growth process as well as extrapolating the experimental procedure to other nanomaterials.

■ ASSOCIATED CONTENT

Ⓢ Supporting Information

Detailed experimental procedures, SEM image of Reuleaux triangle disks stacked vertically, SEM images and XRD spectra of as-prepared products of controlled experiments, and TEM images of hexagonal disks and Reuleaux triangle intermediates. This material is available free of charge via the Internet at http://pubs.acs.org.

■ AUTHOR INFORMATION

Corresponding Author

chmfanwy@nus.edu.sg

Notes

The authors declare no competing financial interest.

■ ACKNOWLEDGMENTS

The project was supported by a National University of Singapore research grant under Grant No. 143-000-553-112. C.H.B.N. thanks NUS for a PGF research scholarship. We thank K. Y. Lee for his support in TEM and SEM microscopy.

■ REFERENCES

(1) Jin, R.; Cao, Y.; Mirkin, C. A.; Kelly, K. L.; Schatz, G. C.; Zheng, J. G. *Science* **2001**, *294*, 1901.
(2) Sun, Y.; Xia, Y. *Science* **2002**, *298*, 2176.
(3) Ahmadi, T. S.; Wang, Z. L.; Green, T. C.; Henglein, A.; El-Sayed, M. A. *Science* **1996**, *272*, 1924.
(4) Xia, Y.; Xiong, Y.; Lim, B.; Skrabalak, S. E. *Angew. Chem., Int. Ed.* **2009**, *48*, 60.
(5) Lim, B.; Xia, Y. *Angew. Chem., Int. Ed.* **2011**, *50*, 76.
(6) Reuleaux, F. *The kinematics of machinery: outlines of a theory of machines*; MacMillan: London, 1876.
(7) Bryant, J.; Sangwin, C. *How round is your circle?: where engineering and mathematics meet*; Princeton University Press: Princeton, NJ, 2008.
(8) Serefis, S. *Arch. Dermatol. Syphilol.* **1934**, *171*, 1.
(9) Ippen, H. *Hautarzt* **1997**, *48*, 424.
(10) Whitehead, M. W.; Phillips, R. H.; Sieniawska, C. E.; Delves, H. T.; Seed, P. T.; Thompson, R.; Powell, J. J. *Helicobacter* **2000**, *5*, 169.
(11) Christensen, A. N.; Chevallier, M. A.; Skibsted, J.; Iversen, B. B. *J. Chem. Soc., Dalton Trans.* **2000**, *3*, 265.
(12) Levy, H. A.; Danford, M. D.; Agron, P. A. *J. Chem. Phys.* **1959**, *31*, 1458.
(13) Henry, N.; Evain, M.; Deniard, P.; Jobic, S.; Mentré, O.; Abraham, F. *J. Solid State Chem.* **2003**, *176*, 127.
(14) Henry, N.; Evain, M.; Deniard, P.; Jobic, S.; Abraham, F.; Mentré, O. *Z. Naturforsch.* **2005**, *60b*, 322.
(15) Jiang, H. H.; Chen, X. Q.; Jiang, X. Y. *Micro Nano Lett.* **2011**, *6*, 196.
(16) Qiu, Y.; Yang, M.; Fan, H.; Zuo, Y.; Shao, Y.; Xu, Y.; Yang, X.; Yang, S. *CrystEngComm* **2011**, *13*, 1843.
(17) Ostwald, W. F. *Phys. Chem.* **1897**, *22*, 289.
(18) Banfield, F.; Welch, S. A.; Zhang, H.; Ebert, T. T.; Penn, R. L. *Science* **2000**, *289*, 751.
(19) Alivisatos, A. P. *Science* **2000**, *289*, 736.
(20) Li, D.; Nielsen, M. H.; Lee, J. R. I.; Frandsen, C.; Banfield, J. F.; De Yoreo, J. J. *Science* **2012**, *336*, 1014.
(21) Hitoshi, K.; Singh, N. H.; Hidetoshi, O.; Shuji, O.; Hiro, M.; Nobutsugu, M.; Atsushi, K.; Katsumichi, O.; Akio, M.; Hachiro, N. *Jpn. J. Appl. Phys.* **1992**, *31*, L1132.
(22) Nalwa, H. S.; Kasai, H.; Okada, S.; Oikawa, H.; Matsuda, H.; Kakuta, A.; Mukoh, A.; Nakanishi, H. *Adv. Mater.* **1993**, *5*, 758.
(23) Suzuki, H. In *Organobismuth Chemistry*; Suzuki, H., Matano, Y., Eds.; Elsevier: Amsterdam, The Netherlands, 2001.
(24) Su, Y.; Yan, X.; Wang, A.; Fei, J.; Cui, Y.; He, Q.; Li, J. *J. Mater. Chem.* **2010**, *20*, 6734.
(25) Han, J. T.; Huang, Y. H.; Huang, W.; Goodenough, J. B. *J. Am. Chem. Soc.* **2006**, *128*, 14454.
(26) Lu, W. G.; Ding, Y.; Chen, Y. X.; Wang, Z. L.; Fang, J. Y. *J. Am. Chem. Soc.* **2005**, *127*, 10112.
(27) Thorneycroft, W. E. *A Text-Book of Inorganic Chemistry*, Friend, J. N., Ed.; Charles Griffin & Company: London, 1936; Vol. *VI*, Part V.
(28) Guo, H.; Chen, Y.; Ping, H.; Wang, L.; Peng, D.-L. *J. Mater. Chem.* **2012**, *22*, 8336.
(29) Maksimuk, S.; Teng, X.; Yang, H. *Phys. Chem. Chem. Phys.* **2006**, *8*, 4660.
(30) Adair, J. H.; Suvaci, E. *Curr. Opin. Colloid Interface Sci.* **2001**, *5*, 160.